Magnetic Superhalogens

DOI: 10.1002/anie.201007205

Manganese-Based Magnetic Superhalogens**

Miao Miao Wu, Haopeng Wang, Yeon Jae Ko, Qian Wang, Qiang Sun, Boggavarapu Kiran, Anil K. Kandalam, Kit H. Bowen, and Puru Jena**

The unusual properties of nanoscale materials brought about by their reduced sizes have ushered in a new era in materials science where materials with tailored properties can be synthesized. A fundamental understanding of how their properties evolve one atom and/or one electron at a time can be best studied with atomic clusters. Numerous studies of clusters over the past 30 years have demonstrated their unique properties, which can be tailored by fixing their size and composition. One of the most important properties of atomic clusters is that they exhibit unusual stability at a specific size and composition. There are two main classes of these stable clusters, which are often referred to as magic clusters. Clusters of simple metals such as sodium exhibit unusual stability at 2, 8, 18, 20, 34, 40, … atoms,[1] while clusters of noble gas atoms exhibit stability at 13, 55, 147, … atoms.[2] The former series is due to electronic shell closure, while the latter is due to atomic shell closure. It has been suggested[3] that magic clusters, owing to their enhanced stabilities, can form building blocks of new cluster assembled materials. Herein we present the discovery of a new class of magnetic magic clusters with molecular composition $(Mn_xCl_{2x+1})^-$ ($x = 1, 2, 3, 4, \ldots$). Supported by photoelectron spectroscopy experiments and density functional theory (DFT)-based calculations, we show that these magic clusters owe their unusual stability neither to the conventional electronic shell closing nor to the atomic shell closing, but to the superhalogen character of their corresponding neutral species and to the d^5 configuration of each of the manganese atoms. These molecular anions have the potential to serve as building blocks of a new class of salts with magnetic and super-oxidizing properties.

$(Mn_xCl_y)^-$ cluster anions were produced in a pulsed-arc cluster ion source[4] and mass analyzed by a time-of-flight (TOF) mass spectrometer. The mass ion intensity distribution is shown in Figure 1. The prominent peaks occur at $MnCl_3^-$,

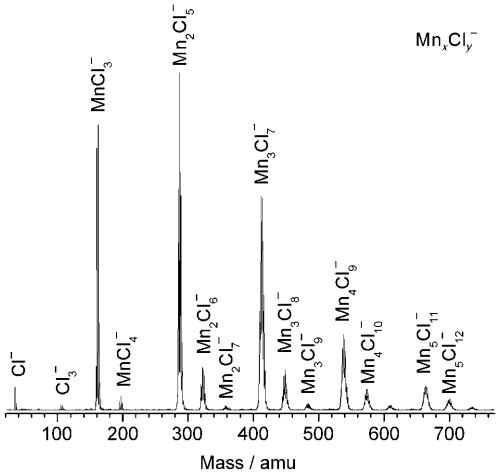

Figure 1. Mass spectra of $Mn_xCl_y^-$ clusters.

$Mn_2Cl_5^-$, $Mn_3Cl_7^-$, and $Mn_4Cl_9^-$, and so on. These clusters have the stoichiometric recursion formula, $(Mn_xCl_{2x+1})^-$ ($x = 1, 2, 3, 4, \ldots$) and in analogy with the prominent peaks observed earlier for alkali metals and noble gas atoms, the prominent peaks in Figure 1 represent magic cluster $(Mn_xCl_{2x+1})^-$ species.

To understand the origin of these peaks, we first note that the most stable oxidation sate for Mn is +2, where the outer $4s^2$ electrons participate in chemical bonding leaving the half-filled $3d^5$ shell to carry a magnetic moment of 5 μ_B. Thus, several Mn^{II} chloride ions are known to exist. If addition of a Cl atom to $MnCl_2$ is considered, an extra electron is necessary to stabilize the $MnCl_3$ moiety as the chlorine atom needs this electron for its electronic shell closure, maintaining the +2 oxidation state and high-spin d^5 configuration of manganese. As we will demonstrate later, this extra electron is now distributed over all three Cl atoms, thus resulting in the high electron affinity (EA) of $MnCl_3$. This follows from the superhalogen model described by Gutsev and Boldyrev some 30 years ago[5,6] and many recent reports.[7–15] Indeed, the electron affinity of $MnCl_3$ measured by Wang and

[*] M. M. Wu, Prof. Q. Wang, Prof. Q. Sun, Prof. P. Jena
Department of Physics, Virginia Commonwealth University
Richmond, VA 23284 (USA)
E-mail: pjena@vcu.edu
M. M. Wu, Prof. Q. Sun
Department of Advanced Materials and Nanotechnology
Peking University
Beijing 100871 (China)
H. Wang, Y. J. Ko, Prof. K. H. Bowen
Department of Chemistry, Johns Hopkins University
Baltimore, MD 21218 (USA)
E-mail: kbowen@jhu.edu
Prof. B. Kiran
Department of Chemistry, McNeese State University
Lake Charles, LA 70609 (USA)
Prof. A. K. Kandalam
Department of Physics, McNeese State University
Lake Charles, LA 70609 (USA)

[**] The work was supported in part by a grant from the Defense Threat Reduction Agency (P.J. and K.H.B.) and in part by the Department of Energy (P.J.).

Supporting information for this article is available on the WWW under http://dx.doi.org/10.1002/anie.201007205.

collaborators[16] is about 5 eV and hence is classified as a conventional superhalogen. To see if the higher $(Mn_xCl_{2x+1})^-$ ($x=2$, 3, 4, …) complexes are also superhalogens, we measured their electron affinities using anion photoelectron spectroscopy (PES).

The PES spectra of $(Mn_xCl_{2x+1})^-$ clusters ($x=1$, 2) is shown in Figure 2. Measured values of adiabatic detachment energy (ADE) and vertical detachment energy (VDE) are presented in Table 1. The photoelectron spectrum of $MnCl_3^-$

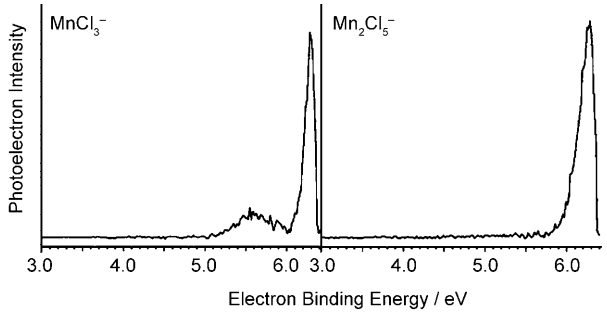

Figure 2. Photoelectron spectra of $Mn_xCl_{2x+1}^-$ clusters ($x=1$, 2).

Table 1: Calculated and measured adiabatic detachment energies (ADE) and vertical detachment energies (VDE) of $Mn_xCl_{2x+1}^-$ clusters ($x=1$–3).

Clusters	ADE [eV] calcd	ADE [eV] expt.	VDE [eV] calcd	VDE [eV] expt.
$MnCl_3^-$	4.82	5.2 ± 0.2	4.94	5.6 ± 0.1
$Mn_2Cl_5^-$	5.68	5.9 ± 0.2	6.17	6.3 ± 0.1
$Mn_3Cl_7^-$	6.06	–	6.74	–

agrees with an earlier experiment.[16] The electron affinity of Mn_2Cl_5 is even higher than that of $MnCl_3$ and thus it too belongs to the superhalogen class. However, Mn_2Cl_5 is not a conventional superhalogen as described by Gutsev and Boldyrev.[5,6] A traditional superhalogen typically consists of a central metal atom surrounded by a halogen (or other electronegative atoms, such as oxygen) and the number of halogen atoms exceeds the valence of the metal atom. There have been a few theoretical predictions[17–19] of multimetal (sp, d^0) fluoride- and chloride-based superhalogens, where each of the metal atoms exists in its maximum oxidation state. In contrast, in the case of Mn_xCl_{2x+1} ($x\geq2$), the superhalogen behavior is attained at the $+2$ oxidation state of Mn, even though Mn can have a maximum oxidation state of $+7$ (MnO_4^- in $KMnO_4$ is an example where the oxidation state of Mn is $+7$).

The superhalogen nature of Mn_xCl_{2x+1} ($x\geq2$) can be understood by considering it as $(MnCl_2)_xCl$ that requires an extra electron to maintain the $+2$ oxidation state of Mn. This extra electron delocalizes over all the chlorine atoms, thus stabilizing the anion. We were unable to photodetach the $(Mn_xCl_{2x+1})^-$ cluster anions ($x\geq3$), indicating that their electron binding energies are higher than 6.4 eV, the upper photon energy available on our excimer laser. These results show that the stabilities of $(Mn_xCl_{2x+1})^-$ clusters originate from two factors: the delocalization of the extra electron over all the available chloride ligands and maintaining the d^5 configuration of Mn in the anion.

To further support and quantify the above hypothesis, we have carried out DFT-based electronic structure calculations of neutral and anionic Mn_xCl_{2x+1} clusters ($x=1$, 2, 3). The vertical and adiabatic detachment energies of the anionic clusters were calculated and compared with the experimentally measured values. If the geometries of neutral and anion clusters do not differ significantly, the measured ADE is considered to be equal to the electron affinity (EA) of the corresponding neutral cluster. A good agreement between these values not only validates the accuracy of the theoretical procedure but also lends confidence to the interpretation of the underlying mechanism for stability.

The lowest-energy isomers of neutral and anionic Mn_xCl_{2x+1} clusters ($x=1$–3), along with the calculated spin magnetic moments, are shown in Figure 3. The charges on each of the atoms were calculated using natural bond orbital (NBO) analysis and are given in the Supporting Information, S1. In the following, we discuss results on each of the Mn_xCl_{2x+1} clusters for $x=1$–3 separately.

The ground-state geometries of neutral and anionic $MnCl_3$ clusters have planar geometries where the chlorine

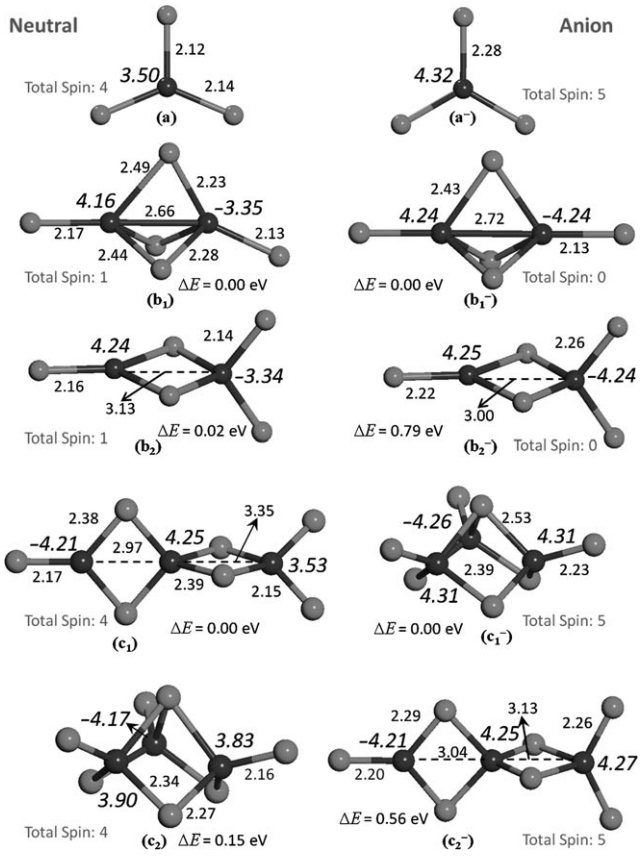

Figure 3. The ground-state geometries of the neutral (a) and anionic (a^-) $MnCl_3$ cluster and the ground-state and higher-energy isomers of the neutral and anionic Mn_2Cl_5 cluster (b_1, b_1^-, b_2, and b_2^-) and the Mn_3Cl_7 cluster (c_1, c_1^-, c_2, and c_2^-). The relative energies and the total spin of each of the clusters is given. The magnetic moments [μ_B] at the Mn site are shown in italics; all bond lengths are given in Å. Mn dark gray, Cl light gray.

binds dissociatively to the central manganese atom (Figure 3). While the anion, $MnCl_3^-$ is symmetric (D_{3h}) with a Mn–Cl bond length of 2.28 Å, the corresponding neutral species is a Jahn–Teller-distorted structure with two different Mn–Cl bond lengths, that is, 2.14 Å and 2.12 Å. The spin multiplicity ($M = 2S + 1$) of $MnCl_3^-$ is a sextet, resulting in total spin magnetic moment of 5 μ_B. As expected, the majority of this moment resides on the 3d states of manganese atom. Similarly, the spin magnetic moment of neutral $MnCl_3$ is 4 μ_B, with a major contribution again coming from the manganese atom. The charge on the manganese atom in neutral $MnCl_3$ cluster is +0.69 e. In $MnCl_3^-$, majority of the charge of the extra electron (83 %) is delocalized over all the three chlorine atoms, while the charge on manganese atom increases slightly to +0.86 e (Supporting Information, S1). The delocalization of the extra electron over three chlorine atoms yields a large value for the calculated electron affinity of $MnCl_3$, namely 4.82 eV. This electron affinity is significantly higher than that of chlorine atom, namely 3.6 eV, and makes $MnCl_3$ a superhalogen. Note that the EA of MnO_4 is also quite large (ca. 5 eV), but unlike in $MnCl_3$, the oxidation sate of Mn in MnO_4^- is +7, thereby making it a non-magnetic superhalogen. The VDE of $MnCl_3^-$ is calculated to be 4.94 eV. This energy corresponds to the detachment of an α electron from the anion and results in neutral cluster with quintet ($2S + 1 = 5$) spin multiplicity. These calculated EA and VDE values are in good agreement with the previous calculations[16] and compare well with our measured values of (5.2 ± 0.2) eV and (5.6 ± 0.1) eV, respectively.

The lowest-energy structures of neutral and anionic Mn_2Cl_5 clusters, given in Figure 3 as b_1 and b_1^-, respectively, are similar to one another, with three of the five chlorine atoms forming a bridge between the two manganese atoms, while the remaining two chlorine atoms bind terminally to each of the manganese atoms. The calculated ADE of Mn_2Cl_5 is 5.68 eV, while the VDE of $Mn_2Cl_5^-$ is calculated to be 6.17 eV. The difference between ADE and VDE values is larger than that in the case of $MnCl_3$, reflecting a larger change in geometry of $Mn_2Cl_5^-$ cluster after electron detachment. The calculated VDE is in very good agreement with the corresponding experimental values of (6.3 ± 0.1) eV. As the neutral and anionic lowest-energy structures are similar, the measured ADE, which is taken as the on-set of electron intensity, is equal to the EA of Mn_2Cl_5.

In the $Mn_2Cl_5^-$ cluster, the manganese atoms prefer an anti-ferromagnetic (AFM) coupling, with spin magnetic moments of +4.24 μ_B and −4.24 μ_B on each of the manganese atoms. This AFM coupling between the manganese atoms results in a singlet spin multiplicity for the anion. The ferromagnetic (FM) state corresponding to this isomer, with a total magnetic moment of 10 μ_B, is 0.26 eV higher in energy than the AFM state. The Mn–Mn bond length in the ground AFM state of the anion is calculated to be 2.72 Å, while in the high-spin FM state the bond length between the metal atoms is 2.89 Å. The Mn–Mn bond length of the Mn_2 dimer in AFM state is 3.4 Å.[20] A second isomer in which only two chlorine atoms are bridging the antiferromagnetically-coupled Mn atoms is found to be 0.79 eV higher in energy than the ground state structure (Figure 3, b_2^-).

The coupling between manganese spin moments in neutral Mn_2Cl_5 is ferrimagnetic, with individual spin magnetic moments of +4.16 μ_B and −3.35 μ_B on each of the manganese atoms. The total spin magnetic moment of Mn_2Cl_5 is 1 μ_B. For this structure, the high-spin FM state with a total moment of 9 μ_B is only 0.13 eV higher in energy than the ferrimagnetic state. However, a second isomer exists with near-identical energy ($\Delta E = 0.02$ eV) in which there are only two bridging chlorine atoms, while one of the manganese atoms binds to two chlorine atoms terminally (Figure 3, b_2). The spin magnetic state of this isomer is also calculated to be 1 μ_B. The FM state (spin magnetic moment = 9 μ_B), corresponding to this higher-energy configuration, is 0.24 eV higher in energy than the ferrimagnetic ground-state configuration.

The ground-state and the higher energy isomers of neutral and anionic Mn_3Cl_7 are also given in Figure 3. Interestingly, ground-state geometries of the neutral and anionic Mn_3Cl_7 clusters completely differ from each other. The neutral Mn_3Cl_7 is an open, linear structure, with only two of the three Mn atoms having four-fold coordination, while the third Mn atom is three-fold coordinated (Figure 3, c_1). This structure can be seen as an extension of the higher energy isomer of neutral Mn_2Cl_5 (Figure 3, b_2). A closed structure, where each of the manganese atoms is bonded to four chlorine atoms, is 0.15 eV higher in energy (Figure 3, c_2). On the other hand, the $Mn_3Cl_7^-$ cluster clearly prefers the closed structure (Figure 3, c_1^-), while the linear structure, which is the ground state in neutral, is 0.56 eV higher in energy (Figure 3, c_2^-).

This switching in the order of the lowest-energy isomers of neutral and anionic Mn_3Cl_7 cluster indicates that the measured ADE is not equal to the EA. The calculated vertical detachment energy (6.74 eV) is significantly larger than that of the VDE of Mn_2Cl_5. As the neutral and anionic geometries of Mn_3Cl_7 differ significantly, we calculated both the electron affinity (EA) and the ADE for this cluster. The EA of Mn_3Cl_7 is calculated to be 5.90 eV, while the ADE of $Mn_3Cl_7^-$ is 6.06 eV. No experimental value could be obtained at the current photon energy, indicating that the ADE of $Mn_3Cl_7^-$ is larger than 6.4 eV. Comparing our calculated results with experimental results of $MnCl_3^-$, we note that this level of theory underestimates the EA. Therefore, the fact that $Mn_3Cl_7^-$ exhibits a prominent peak in the mass spectrum but could not be photodetached is in line with our theoretical prediction. The electron detachment energy values increase with the number of Mn atoms in the $Mn_xCl_{2x+1}^-$ clusters. This trend is consistent with previous studies[13b,19] on $Na_xCl_y^-$, $P_xF_y^-$, and $Ta_xF_y^-$ clusters. The magnetic spin coupling between the manganese atoms in neutral and anionic Mn_3Cl_7 are ferrimagnetic, resulting in total spin magnetic moments of 4 μ_B in Mn_3Cl_7 and 5 μ_B in $Mn_3Cl_7^-$. The moments are almost entirely localized on the manganese atoms. The total charges on the manganese atom in anionic $Mn_3Cl_7^-$ and its corresponding neutral cluster are +1.68 e and +1.26 e, respectively (Supporting Information, S1), indicating that the majority of the charge of the extra electron in $Mn_3Cl_7^-$ is delocalized over seven chlorine atoms, hence the superhalogen behavior of Mn_3Cl_7.

In the above we have demonstrated that a new class of magnetic superhalogens, with a general formula Mn_xCl_{2x+1} ($x = 1, 2, 3$) can be synthesized in which each Mn atom is in a $+2$ state with a high-spin, nearly d^5 configuration. Despite the fact that several $Mn_xCl_y^-$ clusters can potentially form, only the $Mn_xCl_{2x+1}^-$ clusters exhibit the prominent (most abundant) peaks in the mass spectrum. The enhanced stability of these anions is a result of the combination of electron delocalization over chlorine atoms and also the half-filled d shell of Mn atoms. A new class of magic negative cluster ions can be therefore produced by taking advantage of the superhalogen properties of their corresponding neutral species. We should re-emphasize that the Mn_xCl_{2x+1} superhalogens are quite distinct from the conventional superhalogens, where the central core is a single metal atom and the number of halogen atoms surrounding the metal atom exceed its maximal valence by one. Even more important is the fact that Mn_xCl_{2x+1} superhalogens can be magnetic. Thus, a large class of compound magic clusters can now be envisioned where the superhalogen characteristics drive the magicity of their corresponding anions.

As stated above, it has been suggested[3] that owing to their unusual stability, magic clusters can serve as building blocks of bulk materials. We have explored the possibility that the compound clusters discussed above can be used to build crystals. One could envision that a neutral $MnCl_3$ moiety can be further stabilized by interacting it with K and that the resulting compound $K^+MnCl_3^-$ can be as stable as K^+Cl^-. To explore this possibility, we calculated the equilibrium structure and binding energy of $KMnCl_3$. (The calculated ground state geometry of $KMnCl_3$ is given in the Supporting Information, S2.) The geometry of $KMnCl_3$ is planar and the $MnCl_3$ portion of this geometry is almost identical with the geometry of $MnCl_3^-$ given in Figure 3. The binding energy of $KMnCl_3$ against dissociation to K and $MnCl_3$ is 3.67 eV, while that of KCl dissociating to K and Cl is 4.49 eV. To examine whether the formation of $KMnCl_3$ is exothermic or endothermic, we calculated the energy required to fragment $KMnCl_3$ to two stable salts, namely KCl and $MnCl_2$. This fragmentation energy is 1.81 eV; thus, it should be possible to synthesize $KMnCl_3$. We also find that the total magnetic moment of $KMnCl_3$ is 5 μ_B, which is almost entirely located at the manganese site. In analogy with the results of Mn_xCl_{2x+1} ($x = 2, 3$), we can expect that a crystal made of $KMnCl_3$ building blocks will be antiferromagnetic. A search of the literature confirmed our findings: several experimental studies[21,22] exist where $KMnCl_3$ has been synthesized by using KCl and $MnCl_2$ and heating the mixture to a temperature of 500 °C. Neutron-diffraction studies show the structure of $KMnCl_3$ to be a distorted perovskite, which is antiferromagnetic with a magnetic moment of 4.6 ± 0.5 μ_B at the manganese site. Furthermore, the nearest distances of K–Mn and Mn–Cl in $KMnCl_3$ crystal are 4.076 Å and 2.515 Å, respectively. The K–Mn and Mn–Cl bond lengths in crystalline $KMnCl_3$ compares well with those given in the Supporting Information, S2. We have carried out band structure calculations of $KMnCl_3$ and indeed find it to be an antiferromagnetic, with a band gap of 2.31 eV. There has been much interest in the synthesis of magnetic materials from inorganic coordination complexes, such as cyanide-bridged solids[23] formed by treating anionic cyanometalates with transition-metal cations and binuclear chlorine-bridged complexes of Mn^{II} and Ni^{II}.[24]

In conclusion, we have demonstrated that magic clusters whose stability is derived from their superhalogen properties can serve as building blocks of crystals. This may open the door to the synthesis of new salts by finding an appropriate counter ion, say, for Mn_2Cl_5. Using anion photoelectron spectroscopy experiments and density functional theory, we have shown that a new class of magnetic magic clusters, the stabilities of which are governed by the superhalogen behavior and a half-filled d shell, can be designed and synthesized. Although the origin of the superhalogen behavior is due to the closing of the electronic shells of the halogen atoms, this electronic shell closure is different from the electronic shell closure that governs the magicity of the alkali metal clusters. In the latter, all the valence electrons of the cluster participate in a collective filling of the electronic shells of the cluster as a whole, while in the former only the added electron fills the electronic shell of the halogen atoms. The new magnetic superhalogens described here can serve as the building blocks of bulk materials as demonstrated by the case of $KMnCl_3$. This opens the door for focused discovery of many materials with interesting chemistry. Superhalogen building blocks that carry a net magnetic moment provide an additional degree of freedom to design and synthesize new magnetic insulators.

Experimental Section

Negative-ion PES was conducted by crossing a beam of mass selected anions with a fixed-frequency photon beam and analyzing the energy of the resultant photodetached electrons. Our apparatus has been described previously elsewhere.[25] For the current study, 193 nm (6.424 eV) photons from an argon fluoride excimer laser were used for photodetachment. The instrumental resolution of our MB-PES is about 35 meV at EKE = 1 eV, as measured from the spectrum of Cu^- at 355 nm. Photoelectron spectra were calibrated[11] against the transitions of Cu^- and $CuCl_2^-$.

DFT calculations were carried out using generalized gradient approximation (GGA) for the exchange-correlation energy functional. The Perdew–Wang 1991 (PW91) exchange-correlation functional[26] and projector-augmented plane-wave (PAW) basis set as implemented in the Vienna ab initio simulation package (VASP)[27,28] were used. The structure optimization was carried out using conjugate-gradient algorithm without symmetry constraints. The energy cut-off was set to 280 eV, while the convergence for energy and force were set to 10^{-4} eV and 0.005 eV Å^{-1}, respectively. The clusters under investigation were surrounded by 15 Å of vacuum space along the x, y, and z directions, and the Γ point is used to represent the Brillouin zone.

Received: November 16, 2010
Published online: February 10, 2011

Keywords: density functional calculations · magic clusters · magnetic properties · manganese · superhalogens

[1] W. D. Knight, K. Clememger, W. A. de Heer, W. A. Saunders, M. Y. Chou, M. L. Cohen, *Phys. Rev. Lett.* **1984**, *52*, 2141–2143.

[2] O. Echt, K. Sattler, E. Rechnagel, *Phys. Rev. Lett.* **1981**, *47*, 1121 – 1124.
[3] S. N. Khanna, P. Jena, *Phys. Rev. Lett.* **1992**, *69*, 1664 – 1667.
[4] M. Gerhards, O. C. Thomas, J. M. Nilles, W. J. Zheng, K. H. Bowen, *J. Chem. Phys.* **2002**, *116*, 10247 – 10252.
[5] G. L. Gutsev, A. I. Boldyrev, *Chem. Phys.* **1981**, *56*, 277 – 283.
[6] G. L. Gutsev, A. I. Boldyrev, *Chem. Phys. Lett.* **1984**, *108*, 250 – 254.
[7] G. L. Gutsev, A. I. Boldyrev, *J. Phys. Chem.* **1990**, *94*, 2256 – 2258.
[8] M. K. Scheller, R. N. Compton, L. S. Cederbaum, *Science* **1995**, *270*, 1160 – 1166.
[9] a) X. B. Wang, C. F. Ding, L. S. Wang, A. I. Boldyrev, J. Simons, *J. Chem. Phys.* **1999**, *110*, 4763 – 4771; b) B. M. Elliott, E. Koyle, A. I. Bolydrev, X. B. Wang, L. S. Wang, *J. Phys. Chem. A* **2005**, *109*, 11560 – 11567.
[10] a) G. L. Gutsev, B. K. Rao, P. Jena, X. B. Wang, L. S. Wang, *Chem. Phys. Lett.* **1999**, *312*, 598 – 605; b) G. L. Gutsev, P. Jena, H. J. Zhai, L. S. Wang, *J. Chem. Phys.* **2001**, *115*, 7935 – 7944.
[11] X. B. Wang, L. S. Wang, R. Brown, P. Schwerdtfeger, D. Schröder, H. J. Schwarz, *Chem. Phys.* **2001**, *114*, 7388 – 7395.
[12] a) D. Schröder, R. Brown, P. Schwerdtfeger, X. B. Wang, X. Yang, L. S. Wang, H. Schwarz, *Angew. Chem.* **2003**, *115*, 323 – 327; *Angew. Chem. Int. Ed.* **2003**, *42*, 311 – 314; b) B. Dai, J. Yang, *Chem. Phys. Lett.* **2003**, *379*, 512 – 516.
[13] a) A. N. Alexandrova, A. I. Boldyrev, Y. J. Fu, X. Yang, X. B. Wang, L. S. Wang, *J. Chem. Phys.* **2004**, *121*, 5709 – 5719; b) J. Yang, X. B. Wang, X. P. Xing, L. S. Wang, *J. Chem. Phys.* **2008**, *128*, 201102.
[14] Q. Wang, Q. Sun, P. Jena, *J. Chem. Phys.* **2009**, *131*, 124301.
[15] P. Koirala, M. Willis, B. Kiran, A. K. Kandalam, P. Jena, *J. Phys. Chem. C* **2010**, *114*, 16018 – 16024.
[16] X. Yang, X. B. Wang, L. S. Wang, S. Q. Niu, T. Ichiye, *J. Chem. Phys.* **2003**, *119*, 8311 – 8320.
[17] I. Anusiewicz, P. Skurski, *Chem. Phys. Lett.* **2007**, *440*, 41 – 44.
[18] I. Anusiewicz, *Aust. J. Chem.* **2008**, *61*, 712 – 717.
[19] a) C. Kölmel, G. Palm, R. Ahlrichs, M. Bär, A. I. Boldyrev, *Chem. Phys. Lett.* **1990**, *173*, 151 – 156; b) M. Sobczyk, A. Sawicka, P. Skurski, *Eur. J. Inorg. Chem.* **2003**, 3790 – 3797.
[20] C. A. Baumann, R. J. Van Zee, S. V. Bhat, W. Weltner, Jr., *J. Chem. Phys.* **1983**, *78*, 190 – 199.
[21] E. Gurewitz, A. Horowitz, H. Shaked, *Phys. Rev. B* **1979**, *20*, 4544 – 4549.
[22] E. Gurewitz, M. Melamud, A. Horowitz, H. Shaked, *Phys. Rev. B* **1982**, *25*, 5220 – 5229.
[23] W. R. Entley, G. S. Girolami, *Inorg. Chem.* **1994**, *33*, 5165 – 5166.
[24] N. M. Karayannis, C. M. Paleos, L. L. Pytlewski, and M. M. Labes, *Inorg. Chem.* **1969**, *8*, 2559 – 2562.
[25] X. Li, A. Grubisic, S. T. Stokes, J. Cordes, G. F Gantefoer, K. H. Bowen, B. Kiran, M. Willis, P. Jena, R. Burgert, H. Schnoeckel, *Science* **2007**, *315*, 356 – 358.
[26] Y. Wang, J. P. Perdew, *Phys. Rev. B* **1991**, *44*, 13298 – 13307.
[27] P. E. Blöchl, *Phys. Rev. B* **1994**, *50*, 17953 – 17979.
[28] G. Kresse, D. Joubert, *Phys. Rev. B* **1999**, *59*, 1758 – 1775.

